

# RSC Advances



This is an *Accepted Manuscript*, which has been through the Royal Society of Chemistry peer review process and has been accepted for publication.

*Accepted Manuscripts* are published online shortly after acceptance, before technical editing, formatting and proof reading. Using this free service, authors can make their results available to the community, in citable form, before we publish the edited article. This *Accepted Manuscript* will be replaced by the edited, formatted and paginated article as soon as this is available.

You can find more information about *Accepted Manuscripts* in the [Information for Authors](#).

Please note that technical editing may introduce minor changes to the text and/or graphics, which may alter content. The journal's standard [Terms & Conditions](#) and the [Ethical guidelines](#) still apply. In no event shall the Royal Society of Chemistry be held responsible for any errors or omissions in this *Accepted Manuscript* or any consequences arising from the use of any information it contains.

## Nonlinear Optical Properties of Colloidal Carbon Nanoparticles: Nanodiamonds and Carbon Dots

Irene Papagiannouli<sup>a,b</sup>, Athanasios B. Bourlinos<sup>c</sup>, Aristides Bakandritsos<sup>d</sup> and Stelios Couris<sup>a,b\*</sup>

<sup>a</sup>Department of Physics, University of Patras, 26504, Patras, Greece

<sup>b</sup>Institute of Chemical Engineering Sciences (ICE-HT), Foundation for Research and Technology-Hellas (FORTH), 26504, Patras, Greece

<sup>c</sup>Physics Department, University of Ioannina, Ioannina 45110, Greece

<sup>d</sup>Department of Materials Science, University of Patras, Rio 26504, Patra, Greece

\*corresponding author: [couris@iceht.forth.gr](mailto:couris@iceht.forth.gr)

Submitted for publication in *RSC Advances*

August 2014

## Abstract

Colloidal suspensions of nanometer quasi-spherical sized carbon dots and nanodiamonds have been prepared and their third-order nonlinear optical response was investigated by means of the Z-scan technique, employing 35 ps and 4 ns, 1064 and 532 nm laser excitation. Carbon dots were found to exhibit significant nonlinear optical response only under visible excitation for both pulse durations, due entirely to nonlinear refraction. On the other hand, nanodiamonds were found to exhibit significant nonlinear optical response at both excitation wavelengths under ns laser pulses, while in the case of ps excitation, they exhibited sizeable nonlinear optical response only for visible laser pulses. Nevertheless, carbon dots were found to exhibit significantly larger nonlinear optical response than that of nanodiamonds under all experimental conditions examined in the present study. Additionally, the optical limiting behavior of nanodiamonds was investigated in the ns regime, using both visible and infrared laser pulses. Nanodiamonds were found to exhibit important and broadband optical limiting efficiency making them possible candidates for photonic and/or optoelectronic applications.

## 1. Introduction

During the last years the family of nanocarbons has shown a significant growth. Crystalline nanodiamonds (NDs) and amorphous carbon dots (CDs), among others, define a unique class of carbon nanoparticles with fascinating optical properties attracting the interest of the research community in view of their potential application in various fields ranging from photoreduction of metals to light emitters<sup>1,2</sup>. They both belong to the IVA group, along with silicon and germanium-based materials, however, even if they all display semiconducting behavior, the carbonaceous ones exhibit totally different nonlinear optical (NLO) properties<sup>3</sup>.

Although NDs and bulk diamonds have different sizes, the formers exhibiting an average size of less than 12 nm while the latter ones having sizes larger than 30nm, have common characteristics (as e.g., face centered cubic lattice structure, specific surface area, etc.) and similar properties<sup>4</sup>. Diamond-based materials are considered as  $sp^3$  carbon nanomaterials which in the majority of cases, consist of a diamond core (*i.e.*, consisting almost exclusively from carbon, with minimum quantities of hydrogen, oxygen and nitrogen) and small amounts of  $sp^2$  and  $sp^3$  bonded carbon atoms at their surface<sup>5</sup>. In contrast to carbon nanotubes and other allotropes of carbon, NDs offer the possibility of ease functionalization with several functional groups, attached on their surface, which can strongly affect their interactions with solvents and other components, in the case of composite materials, while they can also affect their photostability and fluorescent properties<sup>6-8</sup>. With a broad spectrum of applications, the main of which being in the field of biomedicine, where diamond layers are being used for implants coverage, due to their remarkable bio-tolerance and bio-compatibility with human organism, and most importantly non-toxicity and anti-allergic reaction, NDs dominate over several other materials in this field<sup>9</sup>. Other applications of NDs can be found in biochemistry, for the separation and purification of proteins or even in jewelry industry<sup>10</sup>.

On the other hand, carbonaceous quantum dots, CDs, have a  $sp^2$  character, with less carbon atoms than the NDs and higher oxygen amounts. They also favor surface functionalization and passivation and have found great applicability in bio-imaging due to their low-cost synthesis and low-toxicity, in contrast to semiconducting quantum dots, where heavy metals are involved and thus their use is ambiguous for human

health<sup>11</sup>. Their main characteristic is the shifted emission bands, exhibited for different excitation wavelengths as a consequence of new surface states (*i.e.*, energy levels) formed between the conduction and the valence band, generated and modified by the surface attached species<sup>12,13</sup>. Nevertheless, not only photoluminescence is influenced by these energy traps, but also the NLO properties of CDs, which can be significantly altered by modifying the surface species.

In general, very little is known about the optical nonlinearities of NDs and CDs in the search of novel nonlinear optical materials, complementary to fullerenes, carbon nanotubes or graphenes<sup>14-16</sup>. The present work being among the few existing experimental investigations regarding the NLO response of the above mentioned systems aims to provide a detailed study of the picosecond and nanosecond third-order nonlinear optical nonlinearities of colloidal crystalline NDs and amorphous CDs and examine the similarities and differences of their NLO responses.

## 2. Experimental

### Synthesis and Characterization

Both types of nanoparticles have comparable sizes (<10 nm) and quasi-spherical morphology, with NDs tending to form tight aggregates (100-200 nm) even while being dispersed in a solvent<sup>17,18</sup>. On the other hand, CDs exhibit strong photoluminescent properties originating from complex organic fluorophores embedded in the carbonaceous matrix<sup>2</sup>. In contrast, the NDs used in this study do not display any fluorescence<sup>19</sup>.

In the case of nanodiamonds, 250 mg NDs (Aldrich, 4-6 nm quasi-spherical nanoparticles<sup>19</sup>) was suspended in 50 mL dimethylformamide (DMF, analytical grade) and the mixture was sonicated for 2 h in an ultrasound bath (130 W). The suspension was left in rest for 2-3 days in order to remove any solid particulates prior to collecting the supernatant colloid. In general, DMF is considered a versatile solvent for dispersing various carbon allotropes by mild sonication, including graphene<sup>20</sup>. Graphene monolayers near the boundaries of NDs may further assist the formation of self-stabilized dispersions<sup>21</sup>. Dynamic light scattering (DLS) studies of NDs dispersed in DMF (Fig. 1a) showed the presence of dispersed ND aggregates with an average

hydrodynamic diameter below 200 nm. A very small fraction of aggregates above 200 nm is not excluded though, as the intensity and volume-weighted curves suggest. In case of carbon dots, these were prepared according to a previous method followed by dispersion in water ( $2 \text{ mg mL}^{-1}$ )<sup>22</sup>. The surface of the dots is decorated with pending quaternary ammonium groups [*i.e.*,  $-\text{N}(\text{CH}_3)_3^+$ ] which confer positive surface charge (+43 mV) and high aqueous dispersability towards the formation of ultrastable colloids. CDs show a uniform size/surface charge distribution with an average particle size of 7 nm and quasi-spherical morphology<sup>22</sup>. Based on DLS, CDs do not form aggregates in water as a result of static repulsions. Fig. 2 illustrates schematically the dispersed ND aggregates in DMF as well as the monodispersed CDs in water. Fig. 1B shows a transmission electron microscopy (TEM) image for the dispersed NDs. The TEM of CDs is documented elsewhere<sup>22</sup>.

In order to measure the UV-Vis-NIR absorption spectra of the samples a spectrophotometer (Hitachi U9000) was used, with the suspensions placed in 1 mm optical path length quartz cuvettes. In Fig. 3, the absorption spectra of the samples are presented together with the solvents used (*i.e.* DMF and distilled water). In agreement with previously reported absorption spectra of similar carbon-based nanoparticles, the present spectra were found also to be featureless, the samples being highly transparent in the visible and near-infrared spectral regions<sup>11,12</sup>. In order to ensure the photostability of the samples during the experiments their absorption spectra were routinely checked during the measurements period.

### **Nonlinear optical response**

The third-order NLO properties were investigated by means of the Z-scan technique<sup>23</sup>. Based on the spatial beam-distortion effect, this technique can provide the simultaneous determination of both the nonlinear absorption and refraction of a sample. During this study, two different laser systems have been used, a mode-locked Nd:YAG laser (Quantel YG900) with a pulse duration of 35 ps and a 4 ns Q-switched Nd:YAG laser (EKSPLA NT342), both operating at repetition rate of 1-10 Hz. Z-scan measurements have been performed both at the fundamental wavelength (*i.e.*, 1064 nm) and the second harmonic (at 532 nm) as well. The beam waists (Half Width  $1/e^2$  M) at the focal plane

of the two lasers systems were determined to be 17.4  $\mu\text{m}$  at 532 nm and 30  $\mu\text{m}$  at 1064 nm, when using a 200 mm focal length lens.

The induced nonlinear effects are revealed in the “closed-aperture” and “open-aperture” Z-scan recordings. The former, exhibiting a pre-focal valley followed by a post-focal transmission peak (or vice versa), corresponds to positive (or negative) nonlinear refraction (*i.e.*  $\gamma'$ ,  $\text{Re}\chi^{(3)}$ ), while the latter, displaying a transmission minimum (or maximum) at the focus, corresponds to positive (or negative) nonlinear absorption (*i.e.*  $\beta$ ,  $\text{Im}\chi^{(3)}$ ). Since the “closed-aperture” Z-scan is sensitive to both the nonlinear refraction and absorption, its division by the corresponding “open-aperture” Z-scan, yielding the so-called “divided” Z-scan, allows for the determination of the nonlinear refraction. More details on the technique and the analysis of the experimental data can be found elsewhere<sup>24</sup>.

All Z-scan recordings were normalized and fitted by theoretical expressions of the transmission of a sample exhibiting third-order optical nonlinearities. In this way, the NLO parameters can be obtained. So, by fitting the “open-aperture” normalized Z-scan recording with equation (1) given below, the nonlinear absorption coefficient  $\beta$  can be deduced:

$$T = \frac{1}{\sqrt{\pi} \left( \frac{\beta I_0 L_{\text{eff}}}{1 + z^2/z_0^2} \right)} \int_{-\infty}^{+\infty} \ln \left[ 1 + \frac{\beta I_0 L_{\text{eff}}}{1 + z^2/z_0^2} \exp(-t^2) \right] dt \quad (1)$$

where  $I_0$  is the laser peak intensity at the focus,  $L_{\text{eff}} = (1 - e^{-\alpha_0 L}) / \alpha_0$  is the effective thickness of the sample and  $\alpha_0$  the linear absorption coefficient of the sample.

Next, by fitting the “divided” Z-scan with equation (2):

$$T = 1 - \frac{4\Delta\Phi_0 (z/z_0)^2}{((z/z_0)^2 + 9)((z/z_0)^2 + 1)} \quad (2)$$

the on-axis nonlinear phase-shift at the focus,  $\Delta\Phi_0$ , can be obtained, which is related with the nonlinear refractive index parameter  $\gamma'$  through the equation:

$$\Delta\Phi_0 = kI_0\gamma' L_{\text{eff}} \quad (3)$$

Having determined the nonlinear refractive and absorptive parameters, the real and the imaginary part of the third-order susceptibility  $\chi^{(3)}$  can be easily calculated using the following relations<sup>24</sup>:

$$\text{Re } \chi^{(3)}(esu) = \frac{10^{-6} c(cm/s) n_0^2}{480\pi^2} \gamma'(cm^2W^{-1}) \quad (4)$$

$$\text{Im } \chi^{(3)}(esu) = \frac{10^{-7} c^2 n_0^2}{96\pi^2 \omega} \beta(cmW^{-1}) \quad (5)$$

where  $n_0$  is the refractive index of the solvent,  $\epsilon_0$  is the electric permeability,  $c$  is the speed of light and  $\omega$  is the cyclic frequency of the incident laser beam.

The nonlinear refractive index parameter  $\gamma'$  and the nonlinear refractive index  $n_2$  are related through the relation<sup>23</sup>:

$$n_2(m^2/V^2) = \left[ \frac{c(m/s) n_0 10^{-8}}{360\pi} \right] \gamma'(m^2/W) \quad (6)$$

In order to examine if nonlinear scattering was occurring, a goniometer apparatus was used equipped with a sensitive photodiode capable of moving around the sample. The sample was placed at the focal plane of the laser beam thus experiencing maximum laser intensity. For the range of incident laser intensities employed during the present experiments no significant nonlinear scattering has been observed. Finally, the optical limiting behavior of the samples has been examined by performing energy dependent transmission measurements.

### 3. Results and Discussion

For the Z-scan measurements, different concentration suspensions of the NDs in DMF and of the CDs in distilled water were prepared, all having linear transmittance higher than 60% at 532 nm. In this study, laser pulses of two different temporal durations have been employed ca. 35 ps and 4 ns. The former ones allow for the determination of the electronic NLO response while the latter ones allow the study of the transient NLO response. In order to determine accurately the nonlinear optical parameters of interest (*i.e.*, the nonlinear absorption coefficient  $\beta$  and the nonlinear refractive index parameter  $\gamma'$ ) experiments have been carried out at different incident laser intensities.

Under ps laser excitation, the NDs and CDs suspensions were found to exhibit similar NLO response. In particular, under 1064 nm infrared laser excitation they both exhibited negligible NLO response (*i.e.*, absorption and refraction) for incident laser intensity up to 356 GW/cm<sup>2</sup>, while they exhibited strong nonlinear refraction and

insignificant nonlinear absorption in the visible (*i.e.*, 532 nm). In order to separate the NLO response of the NDs and CDs from that of the solvents used for the suspensions, the response of DMF and distilled water were measured separately. Moreover, in order to avoid the presence of any thermal and/or cumulative effects, the samples were stirred routinely before and after each measurement so that the laser beam was irradiating fresh sample volume each time, while the intensity of the laser beam was kept as low as possible and the repetition rate of the laser was 1 Hz.

Some representative experimental results concerning “divided” Z-scan recordings of the nanocarbons and the solvents, measured with 532 nm laser excitation are shown in Fig. 4. As can be seen, both solvents exhibited important NLO response for the range of laser intensities used. So, their NLO response has been measured and has been removed accordingly from the NLO response of the suspensions. Fig. 4A presents the “divided” Z-scans of neat DMF and of a 0.23 g/ml suspension of NDs in DMF, obtained using the same laser intensity. As shown, the parameter  $\Delta T_{p-v}$  of the solvent was found to be reduced for the suspension, indicating opposite sign NLO refraction. Taking into account that DMF was exhibiting positive NLO refraction, as indicated by its “divided” Z-scan (*i.e.* a pre-focal transmission minimum followed by the post-focal transmission maximum) it results that the NDs should exhibit opposite sign NLO refraction, *i.e.* negative, corresponding to self-defocusing behavior. Similarly, in Fig. 4B, the “divided” Z-scan of an aqueous 2 mg/ml CDs suspension is shown together with that of distilled water measured for the same laser intensity. Again, distilled water was found to exhibit positive NLO refraction, as indicated by its “divided” Z-scan (*i.e.* a pre-focal transmission minimum followed by the post-focal transmission maximum), while the suspension exhibited an opposite behavior *i.e.* a peak-valley configuration. Both experimental evidences suggest that the NDs and the CDs exhibit negative NLO refraction, *i.e.* self-defocusing behavior.

The dependence of the  $\Delta T_{p-v}$  parameter (*i.e.* the difference of the normalized transmission between the peak and the valley) upon the energy of the incident laser beam is depicted in Fig. 5 for both nanocarbons. From the slopes of the solid lines corresponding to the linear best fits of the experimental data shown in Fig. 5A and 5B, the nonlinear refractive index parameter  $\gamma'$  can be deduced. Then, using the formulas (4)-(6), the nonlinear refractive index  $n_2$ , the real part and the magnitude of the third-order susceptibility  $\chi^{(3)}$  have been calculated. The determined values are reported in

Table 1. Since the third-order susceptibility is a concentration dependent quantity, in order to facilitate comparison with other materials exhibiting NLO response, the  $\chi^{(3)}/C$  has been also calculated and given in this table. From the comparison of the  $\chi^{(3)}/C$  values of the NDs and CDs, it becomes obvious that CDs exhibit almost 200 times higher nonlinearity than their counterparts NDs. The  $\chi^{(3)}$  values of DMF and distilled water have been found to be in good agreement with other literature reported values<sup>25</sup>.

In the case of nanosecond excitation though, the nanocarbons exhibited totally different behavior. Again, Z-scan measurements have been performed for different concentrations and various laser energies, under 532 and 1064 nm laser excitation conditions. Moreover, the solvents did not display any NLO response for the range, at least, of incident laser intensities, *i.e.* up to  $I_0=0.8$  GW/cm<sup>2</sup>. Therefore, the NLO response exhibited by the suspensions was exclusively due to the carbonaceous materials.

In Fig. 6, the variation of the  $\Delta T_{p-v}$  parameter as a function of the laser energy of some NDs suspensions is presented. In the insets, some representative “closed-” and “open-aperture” Z-scans, obtained under visible and infrared laser excitation, are also shown. As can be seen, the NDs, at both excitation wavelengths, exhibited reverse saturable absorption (RSA) and self-defocusing behavior as indicated by the transmission minimum and the peak-valley configuration displayed by the corresponding “open-” and “closed-aperture” Z-scans. It should be noted at this point that NDs exhibited similar NLO response under 532 and 1064 nm. In fact, the corresponding  $\chi^{(3)}/C$  values revealed stronger NLO response in the infrared than in the visible, a finding of particular interest for several applications including telecommunications.

As far as it concerns the CDs now, under 532 nm laser excitation, they were found to possess negative nonlinear refraction (*i.e.*, self-defocusing behavior), similar to the NDs, while they did not exhibit any nonlinear absorption for the range of incident laser intensities employed. Nevertheless, the calculated  $\chi^{(3)}/C$  values of the CDs were found to be two orders of magnitude larger than those of NDs. In addition, CDs were found to exhibit negligible nonlinear absorption and refraction under 1064 nm excitation. The observed differences in the NLO response of the two nanocarbons can be understood in terms of the different structure of the nanocrystalline NDs and the amorphous CDs. So, due to different hybridizations of the two nanocarbons and their surface

functionalities, the  $sp^2/sp^3$  ratio and consequently their band gaps should be different. These factors are associated with the significant variations of the NLO response of organic materials with semiconducting behavior, thus providing a way of tailoring their properties and applicability<sup>26,27</sup>.

According to some previous studies, the NLO response of similar carbonaceous systems under ns excitation was often associated with bubbles' formation and the presence of important nonlinear scattering<sup>28-30</sup>. In order to provide more insight into this direction, further measurements were performed aiming to search for such effects under the present experimental conditions. For this purpose, a sensitive photodiode has been used, mounted on a goniometric table, while the cell containing the sample was positioned at the focal level of the laser beam. The photodiode was able to move freely around the sample, detecting any scattered light with good sensitivity. As an example, two such recordings are depicted in Fig. 7, obtained under two different laser intensities corresponding to those used during Z-scan measurements. As shown, for both intensities, measurable signal was found only for a narrow angular range around the beam propagation axis (i.e., less than  $\pm 10^\circ$ ) indicating the absence of scattered light, while some weak scattering appeared at  $\pm 10^\circ$  (see e.g. inset of Fig. 7) at much higher incident intensity (e.g.,  $0.9 \text{ GW/cm}^2$ ) than that used for the NLO experiments ( $57\text{-}350 \text{ MW/cm}^2$ ) is attributed to weak nonlinear scattering.

Similar studies on other carbon nanomaterials, have revealed the presence of important nonlinear scattering. For example, in a study investigating some onion-like carbon nanoparticles and some diamond nanoparticles under 10 ns, 532 nm laser pulses, it was found that their NLO response was due to nonlinear scattering<sup>28</sup>. More in detail, both types of nanoparticles exhibited positive nonlinear absorption and negligible nonlinear refraction, while the optical limiting (OL) performance of onion-like carbon nanoparticles was found to be better than that of diamond nanoparticles. Moreover, in agreement with the present findings, the onion-like carbon nanoparticles were found to exhibit much stronger NLO response than the NDs, the corresponding nonlinear absorption coefficients  $\beta$  being  $2 \times 10^{-9}$  and  $30 \times 10^{-11} \text{ m/W}$  respectively. In fact, the reported value for the NDs is close enough to the value determined here, although much higher laser intensities (i.e., higher than  $120 \text{ MW/cm}^2$ ) have been employed in reference [28] than in the present study.

As it is known, nonlinear scattering depends strongly on the size of the nanoparticles<sup>29,30</sup>. So, different size NDs investigated by 17 ns, 532 nm laser excitation have been found to exhibit very important variation of their OL efficiency, the OL threshold decreasing as the size of the diamond nanoparticles was increasing, due to more intense nonlinear scattering. In fact, it was reported that nonlinear scattering was dominant for nanoparticles having size from 50 to 320 nm (*i.e.*, Rayleigh scattering).

Fig. 8 presents the variation of the output fluence as a function of the input fluence for some NDs suspensions both for visible and infrared laser radiations. So, in Fig. 8A, the optical limiting behavior of a 0.23 g/ml suspension of NDs in DMF is shown, having a linear transmittance of  $T=50\%$  at 532 nm. The input fluence at which the transmittance starts deviating from the normalized linear transmittance represented by the dashed line, *i.e.*, the OL onset, was determined to be about  $0.25 \text{ J/cm}^2$ . For comparison, the optical limiting action of a  $\text{C}_{60}$ -toluene solution having similar linear transmission is also shown in the same graph, the selection of  $\text{C}_{60}$  being based on the fact that it is well known for his excellent optical limiting properties. As shown, they were both found to exhibit similar OL onsets, suggesting that NDs is at least as good as fullerenes. The onset value determined here is however significantly lower than that reported in references<sup>29,30</sup>, lying between  $1.1$  and  $4.5 \text{ J/cm}^2$ . The main cause of this difference could be the significantly larger size of nanoparticles (50-320nm) favoring important nonlinear scattering to occur, resulting to optical limiting. Instead of nonlinear scattering, the nonlinear absorptive behavior of the present NDs, can be related to excited-state absorption (ESA) mechanisms, which are known to enhance the nonlinear absorption and therefore to favour the optical limiting response of carbon-based materials (*i.e.*, CDs, carbon nanotubes and graphene oxides in the ns timescale)<sup>16,31-33</sup>. Other mechanisms such as two-photon absorption should not be considered in the ns regime, since they can be achieved by incident intensities of the order of  $\text{GW/cm}^2$  or higher, for instance under ps or fs laser pulses. Furthermore, under ps excitation, free-carrier absorption (FCA) has been proposed as possible mechanism<sup>34</sup>. In fact, transient transmission measurements performed on some onion-like carbon nanostructures under 10 ps, 400 nm excitation, have shown that the effect of photo-generated carriers is dominant for probing wavelengths in the spectral range 550-1000 nm<sup>34</sup>, evidencing that FCA is indeed an operating mechanism for optical limiting.

Under 1064 nm laser excitation conditions, the same suspension of NDs, exhibiting a linear transmittance of  $T=75\%$  at 1064 nm, has also shown important OL action, its onset being about  $0.5 \text{ J/cm}^2$ . Based on the results reported in Table 2 and Fig. 8B for the infrared excitation, it becomes evident that enhancement of NLO response is not always accompanied by decrease of the OL onset. Finally, one should recall that under 1064 nm irradiation,  $\text{C}_{60}$  did not exhibit any nonlinear absorption and OL action. Hence, it can be concluded that NDs compared to fullerenes exhibit certainly more broadband and powerful OL action. Recently, in a study of some other NDs produced by detonation techniques, using 7 ns, 1064 nm laser pulses, it was shown that their OL efficiency was directly correlated with the polydispersity of the suspensions, which are influencing the Rayleigh scattering and hence the OL properties<sup>35</sup>. Such behavior was also confirmed in the present work, although pertaining to different type of NDs and studied at different conditions (4 ns pulses).

Apart from the optical limiting behavior of NDs, their third-order NLO properties have been mainly investigated using femtosecond excitation<sup>36-38</sup>. For instance, Kozak *et al.* examined the nonlinear absorption and refraction of monocrystalline chemical vapor deposition diamond by fs Z-scan for various photon energies, smaller and larger than the indirect bandgap of diamond (*i.e.*, 5.5 eV) and they have found RSA and self-focusing behavior<sup>39</sup>. The values of two-photon absorption and the nonlinear refractive index parameter were determined to be  $0.9 \times 10^{-11} \text{ m/W}$  and  $8 \times 10^{-20} \text{ m}^2/\text{W}$ , at 4 eV and 2.9 eV, respectively. In two other similar studies by the same group, nanocrystalline diamonds were found to have similar NLO responses with bulk diamond under fs laser excitation<sup>36,40</sup>. Nevertheless, in all cases,  $\chi^{(3)}$  values of the order of  $10^{-13} \text{ esu}$  have been reported, yet, no direct comparison between these values and those determined here can be done, since different laser pulse durations have been employed in each case. Under ps laser excitation, natural diamond (IIa type) when excited with 532 nm exhibits negligible absorption and measurable nonlinear refraction, whereas the nonlinear refractive index parameter was found to be  $0.07 \times 10^{-18} \text{ m}^2/\text{W}$  for incident intensities comparable with those used in our experiments (*i.e.*,  $50 \text{ GW/cm}^2$ ). This value is relatively close to the values reported in Table 1, indicating similar NLO response between bulk and nanocolloidal diamonds in the ps regime<sup>37</sup>.

The NLO properties of CDs, on the other hand, were less investigated until recently<sup>41,42</sup>. Most of the previous works have reported on the optical limiting of carbon

nanoparticles and onion-like carbons resulting from light scattering caused either by nanobubbles and/or vapor shell around the particles due to heating<sup>28,38,43-46</sup>. Another type of carbon dots, namely some organophilic and hydrophilic amorphous CDs, with sizes 3-15 nm, derived from gallate precursors, have shown significant differences in their NLO response under 4 ns laser excitation<sup>42</sup>. Specifically, the organophilic CDs, exhibited SA to RSA behavior with increasing intensity under 532 nm and SA under 1064 nm, whereas the hydrophilic ones exhibited RSA when excited with visible excitation and negligible nonlinear absorption under infrared light. On the other hand, the CDs studied here, derived from “tris” and betaine precursors and expressing ammonium surface groups,<sup>22</sup> were found exhibiting negligible nonlinear absorption. As shown, the various surface attached groups are greatly affecting the nonlinear absorption of the colloidal dispersions. However, under ps laser excitation, the CDs studied here and the CDs of reference<sup>42</sup> were found to have similar NLO characteristics, exhibiting self-defocusing behavior and negligible nonlinear absorption, under 532 nm laser excitation and insignificant NLO response at 1064 nm. Regarding the CDs’ third-order susceptibility  $\chi^{(3)}$  values, the presently studied CDs were found to exhibit higher  $\chi^{(3)}$ , for similar concentrations, than both their organophilic and hydrophilic counterparts by two orders of magnitude. On the other hand, some onion-like carbon structures, investigated using 10 ns, 532 nm were characterized by negligible nonlinear refraction and sizeable RSA behavior, their response arising from intense nonlinear scattering. Therefore, for the consideration of the NLO response of such carbon based nanomaterials, several parameters should be taken into account, such as the particle size, surface passivation, the nature of organic moieties used, as well as the electronic band structure of the material.

This study, except for adding new experimental results, also constitutes an important review of CDs and NDs, summarizing all the available experimental results in the literature up to now. Generally, carbon nanomaterials exhibit a large third-order nonlinear optical response, ranging from  $10^{-11}$  to  $10^{-13}$  esu<sup>16,24,42</sup>. In the present work we have demonstrated that not only CDs, but also nanodiamonds can compete quite well with established carbon materials, in terms of their NLO response and related properties. Furthermore, parameters like particle size, composition, surface passivation and organic precursor have been shown to further improve these properties, leading to the creation of even more effective carbon-based optical limiters.

## 4. Conclusions

In conclusion, crystalline NDs and amorphous CDs suspensions were prepared and their third-order NLO response has been investigated by using 532 and 1064 nm, ps and ns laser pulses. In all cases, the colloidal suspensions exhibited important NLO response. In particular, CDs were found to exhibit strong nonlinear refraction (self-defocusing) and negligible nonlinear absorption under visible, ps and ns excitation and insignificant response under infrared excitation. On the other hand, NDs exhibited self-defocusing behavior both for visible and infrared excitation, while under ns excitation positive nonlinear absorption (RSA) was also present, the origin of which being related to excited state absorption. Moreover, the optical limiting action of the NDs has been studied for ns pulses. The OL threshold of NDs was determined to be about 0.25 and 0.5 J/cm<sup>2</sup> for 532 and 1064 nm pulses respectively. Finally, it was found that CDs exhibited an almost two orders of magnitude higher NLO response than NDs. The present results provide new useful information about the NLO properties of nanometer size CDs and diamonds in particular for designing nanocarbon based optical limiting devices and for various other photonic applications.

## Acknowledgements

IP and SC acknowledge partial support by the European Union (European Social Fund–ESF) and Greek national funds through the Operational Program "Education and Lifelong Learning" of the National Strategic Reference Framework (NSRF)-Research Funding Programs: Heracleitus II: Investing in knowledge society through the European Social Fund.

## References

1. V. N. Mochalin, O. Shenderova, D. Ho and Y. Gogotsi, *Nature Nanotechnol.*, 2012, **7**, 11.
2. S. N. Baker and G. A. Baker, *Angew. Chem. Int. Ed.*, 2010, **49**, 6726.
3. K. Jarasiunas, R. Aleksiejunas, T. Malinauskas, S. Nargelas and P. Scajev, *Mater. Res. Soc. Symp. Proc.*, 2012, **1396**, 147.
4. V. Yu Dolmatov, *Russ. Chem. Rev.*, 2007, **76**, 339.
5. A. E. Aleksenskii, M. V. Baïdakova, A. Ya, Vul' and V. I. Siklitskii, *Phys. Solid State*, 1999, **41**, 668.
6. A. M. Schrand, S. A. C. Hens and O. A. Shenderova, *Crit. Rev. Solid state Mater. Sci.*, 2009, **34**, 18.
7. L. C. L. Huang and H. C. Chang, *Langmuir*, 2004, **20**, 5879.
8. V. N. Mochalin and Y. Gogotsi, *J. Am. Chem. Soc.* 2009, **131**, 4594.
9. S. Mitura, K. Mitura, P. Niedzielski, P. Louda, V. Danilenko, *Journal of achievements in materials and manufacturing engineering*, 2006, **16**, 9.
10. M. Clapa, S. Mitura, P. Niedzielski, A. Mitura and J. Hassard, *Diamond Rel. Materials*, 2001, **10**, 1121.
11. S. N. Baker and G.A. Baker, *Angew. Chem. Int. Ed.*, 2010, **49**, 6726.
12. A. B. Bourlinos, A. Stassinopoulos, D. Anglos, R. Zboril, V. Georgakilas and E. P. Giannelis, *Chem, Mater.*, 2008, **20**, 4539.
13. H. Peng and J. Travas-Sejdic, *Chem. Mater.*, 2009, **21**, 5563.
14. I. Fuks-Janczarek, S. Dabos-Seigna, B. Sahraoui, I. V. Kityk, J. Berdowski, E. Allard and J. Cousseau, *Opt. Commun.*, 2002, **211**, 303.
15. S. Chu, S. Wang and Q. Gong, *Chem. Phys. Lett.*, 2012, **523**, 104.
16. N. Liaros, P. Aloukos, A. Kolokithas-Ntoukas, A. Bakandritsos, T. Szabo, R. Zboril and S. Couris, *J. Phys. Chem. C*, 2013, 117, 6842.
17. E. Osawa, *Diam. Relat. Mater.*, 2007, **16**, 2018.
18. A. S. Barnard, *J. Mater. Chem.*, 2008, **18**, 4038.

19. A. B. Bourlinos, R. Zboril, M. Kubala, P. Stathi, Y. Deligiannakis, M. A. Karakassides, T. A. Steriotis and A. K. Stubos, *J. Mater. Sci.*, 2011, **46**, 7912.
20. A.B. Bourlinos, V. Georgakilas, R. Zboril, T. A. Steriotis and A. K. Stubos, *Small*, 2009, **5**, 1841.
21. J.-Y. Raty, G. Galli, C. Bostedt, T. W. Van Buuren and L. J. Terminello, *Phys. Rev. Lett.*, 2003, **90**, 037401/1.
22. A. B. Bourlinos, R. Zboril, J. Petr, A. Bakandritsos, M. Krysmann and E. P. Giannelis, *Chem. Mater.*, 2012, **24**, 6
23. M. Sheik-Bahae, A. A. Said, T. Wei, D.J. Hagan and E.W. Stryland, *IEEE J. Quant. Electr.*, 1990, **26**, 760.
24. S. Couris, E. Koudoumas, A.A. Ruth and S. Leach, *J. Phys. B: At. Mol. Opt. Phys.*, 1995, **28**, 4537.
25. P. P. Ho and R. R. Alfano, *Phys. Rev. A*, 1979, **20**, 2170.
26. N. Liaros, A. B. Bourlinos, R. Zboril and S. Couris, *Opt Express*, 2013, **21**, 21027.
27. S. K. O' Leary, *Appl Phys Lett*, 1998, **72**, 1332.
28. E. Koudoumas, O. Kokkinaki, M. Konstantaki, S. Couris, S. Korovin, P. Detkov, V. Kuznetsov, S. Pimenov and V. Pustovoi, *Chem. Phys. Lett.*, 2002, **357**, 336.
29. G. M. Mikheev, A. P. Puzyr', V. V. Vanyukov, T. N. Mogileva and V.S. Bondar, *Tech. Phys. Lett.*, 2013, **39**, 229.
30. V. Vanyukov, T. Mogileva G. Mikheev, , A. Puzir, V. Bondar and Y. Svirko, *Appl. Optics*, 2013, **52**, 4123.
31. B. Anand, R. Podila, P. Ayala, L. Oliveira, R. Philip, S. S. Sankara Sai, A. A. Zakhidov and A. M. Rao, *Nanoscale*, 2013, **5**, 7271.
32. J. Wang, K.-S. Liao, D. Fruchtl, Y. Tian, A. Gilchrist, N. J. Alley, E. Andreoli, B. Aitchison, A. G. Nasibulin, H. J. Byrne, E. I. Kauppinen, L. Zhang, W. J. Blau and S. A. Curran, *Mater. Chem. Phys.*, 2012, **133**, 992.

33. Z. Liu, Y. Wang, X. Zhang, Y. Xu, Y. Chen and J. Tian, *Appl. Phys. Lett.*, 2009, **94**, 021902.
34. M. Pervolaraki, Ph. Komninou, J. Kioseoglou, A. Othonos and J. Giapintzakis, *Appl Surf Sci* 2013, **278**, 101.
35. S. Josset, O. Muller, L. Schmidlin, V. Pichot and D. Spitzer, *Diam. Relat. Mater.*, 2013, **32**, 66.
36. F. Trojanek, K. Zidek, B. Dzurnak, M. Kozak and P. Maly, *Opt. Express*, 2010, **18**, 1349.
37. M. Sheik-Bahae, R. DeSalvo, A. A. Said, D. J. Hagan, M. J. Soileau and E. W. Stryland, Proceedings of SPIE-The international society for optical engineering, 1995, **2428**, 605.
38. D. Li, Y. Liu, H. Yang and S. Qian, *Appl. Phys. Lett.*, 2002, **81**, 2088.
39. M. Kozak, F. Trojanek, B. Dzurnak and P. Maly, *J. Opt. Soc. Am. B*, 2012, **29**, 1141.
40. M. Kozak, F. Trojanek, B. Rezek, A. Kromka and P. Maly, *Physica E*, 2012, **44**, 1300.
41. A. B. Bourlinos, M. A. Karakassides, A. Kouloumpis, D. Gournis, A. Bakandritsos, I. Papagiannouli, P. Aloukos, S. Couris, K. Hola, K. Safarova, R. Zboril, M. Krysmann and E. P. Giannelis, *Carbon*, 2013, **61**, 640.
42. P. Aloukos, I. Papagiannouli, A. B. Bourlinos, R. Zboril, S. Couris, *Opt. Express*, 2014, **22**, 12013.
43. G. X. Chen, M. H. Hong, L. S. Tan, T. C. Chong, H. I. Elim, W. Z. Chen and W. Ji, *J. Phys. Conf. Ser.*, 2007, **59**, 289.
44. I. M. Belousova, N. G. Mironova, A. G. Scobelev and M. S. Yur'ev, *Opt. Commun.*, 2004, **235**, 445.
45. S. Hu, Y. Dong, J. Yang, J. Liu and S. Cao, *J. Mater. Chem.*, 2012, **22**, 1957.
46. G. X. Chen, M. H. Hong, T. S. Ong, H. M. Lam, W. Z. Chen, H. I. Elim, W. Ji and T. C. Chong, *Carbon*, 2004, **42**, 2735.

**Table 1** Nonlinear optical parameters of NDs and CDs determined under 35 ps, 532 nm laser excitation.

	<b>C</b> (g/ml)	$\gamma'$ ( $\times 10^{-18} \text{ m}^2/\text{W}$ )	$n_2$ ( $\times 10^{-22} \text{ m}^2/\text{V}^2$ )	$\chi^{(3)}$ ( $\times 10^{-13} \text{ esu}$ )	$\chi^{(3)}/C$ ( $\times 10^{-13} \text{ esu ml/g}$ )
NDs	0.23	-0.28 $\pm$ 0.01	-10.6 $\pm$ 0.4	0.36 $\pm$ 0.02	1.44 $\pm$ 0.12
	0.15	-0.14 $\pm$ 0.01	-5.3 $\pm$ 0.4	0.18 $\pm$ 0.01	
	0.10	-0.1 $\pm$ 0.01	-3.8 $\pm$ 0.4	0.13 $\pm$ 0.01	
DMF		0.48 $\pm$ 0.02	18.2 $\pm$ 0.8	0.62 $\pm$ 0.02	
	<b>C</b> (mg/ml)	$\gamma'$ ( $\times 10^{-18} \text{ m}^2/\text{W}$ )	$n_2$ ( $\times 10^{-22} \text{ m}^2/\text{V}^2$ )	$\chi^{(3)}$ ( $\times 10^{-13} \text{ esu}$ )	$\chi^{(3)}/C$ ( $\times 10^{-11} \text{ esu ml/g}$ )
CDs	2	-0.43 $\pm$ 0.03	-15.2 $\pm$ 1.0	0.48 $\pm$ 0.04	2.6 $\pm$ 0.2
	1.3	-0.33 $\pm$ 0.02	-11.6 $\pm$ 0.7	0.37 $\pm$ 0.03	
	0.9	-0.27 $\pm$ 0.02	-9.5 $\pm$ 0.7	0.30 $\pm$ 0.02	
H <sub>2</sub> O		0.17 $\pm$ 0.02	-6.0 $\pm$ 0.7	0.14 $\pm$ 0.08	

**Table 2** Nonlinear optical parameters of NDs and CDs determined under 4 ns, 532 nm laser excitation.

<b>C</b> (g/ml)	<b><math>\beta</math></b> ( $\times 10^{-11}$ m/W)	<b><math>\gamma'</math></b> ( $\times 10^{-18}$ m <sup>2</sup> /W)	<b><math>n_2</math></b> ( $\times 10^{-20}$ m <sup>2</sup> /V <sup>2</sup> )	<b><math>\chi^{(3)}</math></b> ( $\times 10^{-13}$ esu)	<b><math>\chi^{(3)}/C</math></b> ( $\times 10^{-11}$ esu ml/g)
<b>NDs, 532 nm</b>					
0.23	27.2 $\pm$ 5.8	-15.4 $\pm$ 3.8	-5.8 $\pm$ 1.4	24.6 $\pm$ 5.2	1.0 $\pm$ 0.1
0.15	7.2 $\pm$ 0.5	-10.2 $\pm$ 1.1	-3.9 $\pm$ 0.4	13.8 $\pm$ 1.4	
<b>NDs, 1064 nm</b>					
0.33	65.3 $\pm$ 10.5	-42.2 $\pm$ 5.6	-16.0 $\pm$ 2.1	90.2 $\pm$ 13.7	3.1 $\pm$ 0.3
0.23	57.5 $\pm$ 18.7	-33.8 $\pm$ 12.5	-12.8 $\pm$ 4.7	77.0 $\pm$ 22.5	
0.15	38.9 $\pm$ 9.5	-27.5 $\pm$ 6.3	-10.4 $\pm$ 2.4	55.6 $\pm$ 13.4	
0.10	34.2 $\pm$ 6.3	-20.7 $\pm$ 8.1	-7.8 $\pm$ 0.3	46.2 $\pm$ 12.6	
<b>CDs, 532 nm</b>					
<b>C</b> (mg/ml)	<b><math>\beta</math></b> ( $\times 10^{-11}$ m/W)	<b><math>\gamma'</math></b> ( $\times 10^{-18}$ m <sup>2</sup> /W)	<b><math>n_2</math></b> ( $\times 10^{-20}$ m <sup>2</sup> /V <sup>2</sup> )	<b><math>\chi^{(3)}</math></b> ( $10^{-13}$ esu)	<b><math>\chi^{(3)}/C</math></b> ( $10^{-9}$ esu $\times$ ml/g)
2	-	-9.8 $\pm$ 1.5	-3.4 $\pm$ 0.5	11.3 $\pm$ 1.8	0.6 $\pm$ 0.1
1.3	-	-5.4 $\pm$ 0.9	-1.9 $\pm$ 0.3	7.2 $\pm$ 1.1	

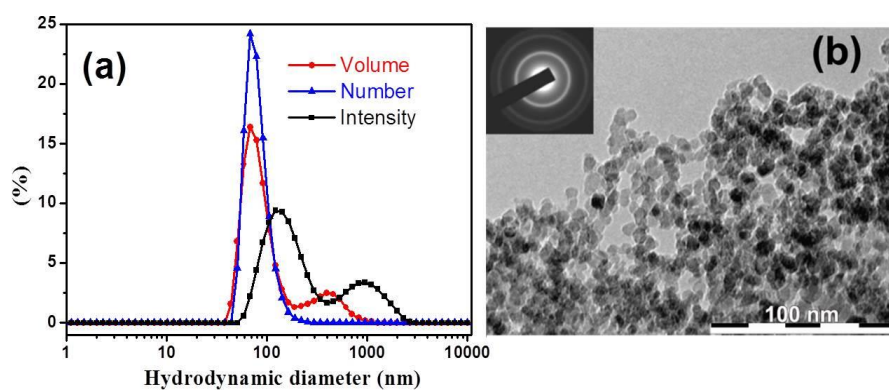


**Fig. 1** Distribution of the hydrodynamic diameter of crystalline NDs dispersed in DMF expressed in terms of scattered light intensity volume and number. (b) Image acquired with TEM.

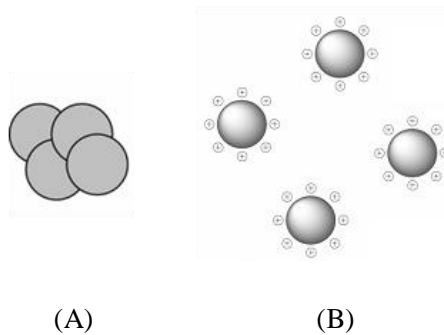


**Fig. 2** Illustrative scheme of the dispersed ND aggregates in DMF (A) and monodisperse CDs in water (B). The surface of CDs is positively charged (+43 mV) providing static repulsions.

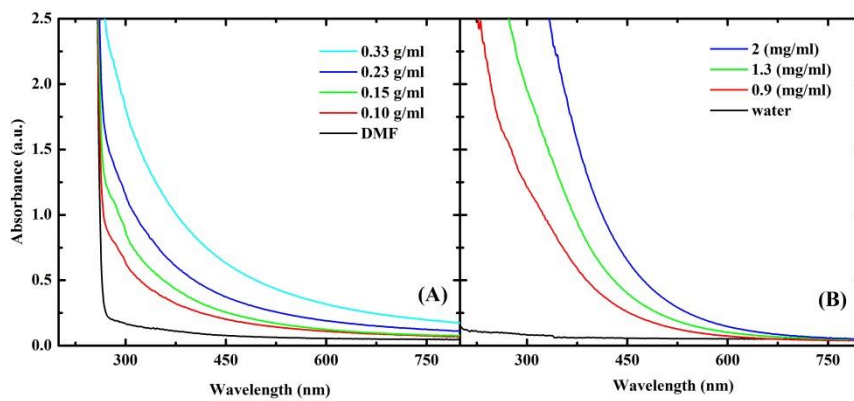


**Fig. 3** Optical absorption spectra of some suspensions of NDs in DMF (A) and CDs in water (B).

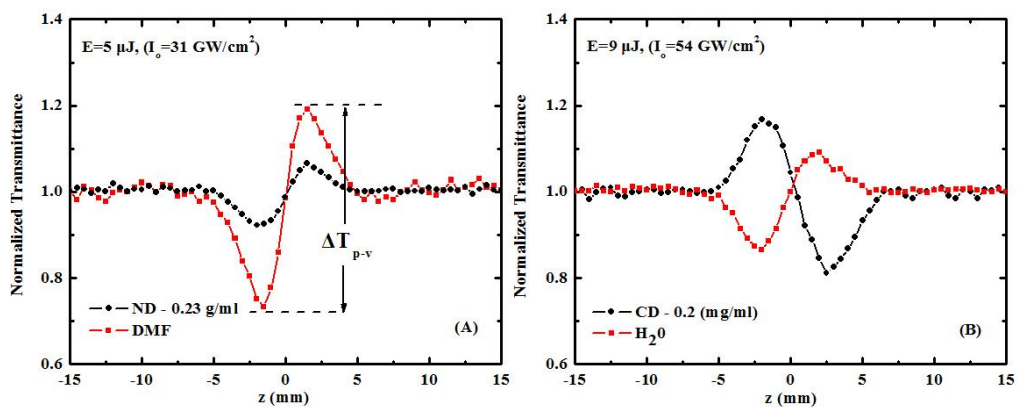


**Fig. 4** “Divided” Z-scans of DMF and a 0.23g/ml suspension of NDs in DMF (A), water and a 2 mg/ml suspension of CDs in water (B).

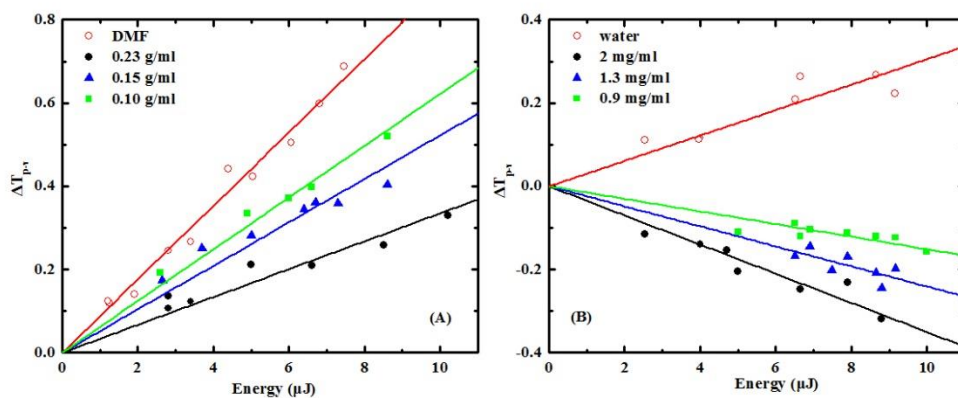


**Fig. 5**  $\Delta T_{p-v}$  variation versus laser energy for some suspensions of: NDs in DMF (A) and CDs in distilled water (B), both obtained under 35 ps, 532 nm.

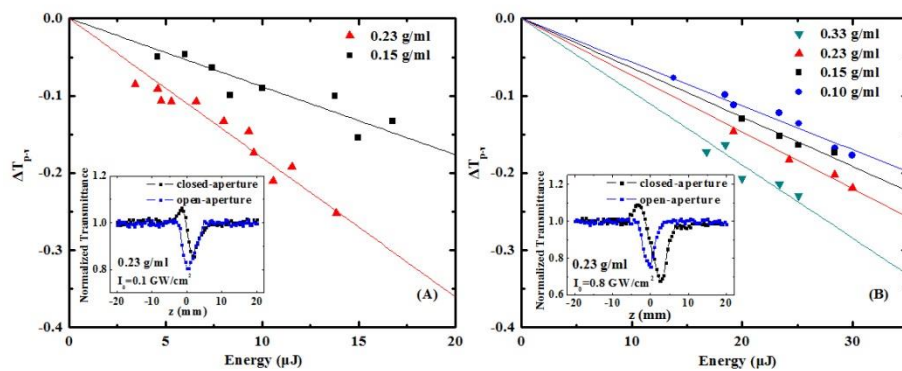


**Fig. 6** Energy dependence of the  $\Delta T_{p-v}$  for NDs, obtained under (A) 532 nm and (B) 1064 nm, 4ns laser excitation. In the insets, some “closed-” and “open-aperture” Z-scans are shown.

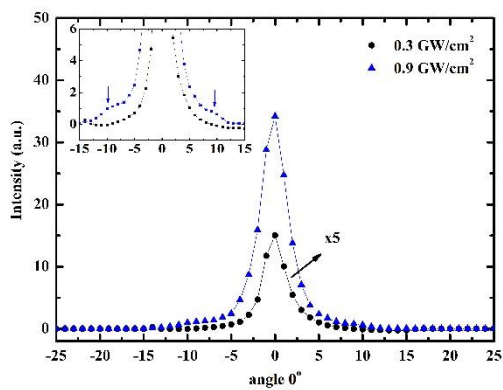


**Fig. 7** Angular distribution of the laser light transmitted through a 0.33 g/ml suspension of NDs, under 4 ns, 532 nm laser light at two different intensities.

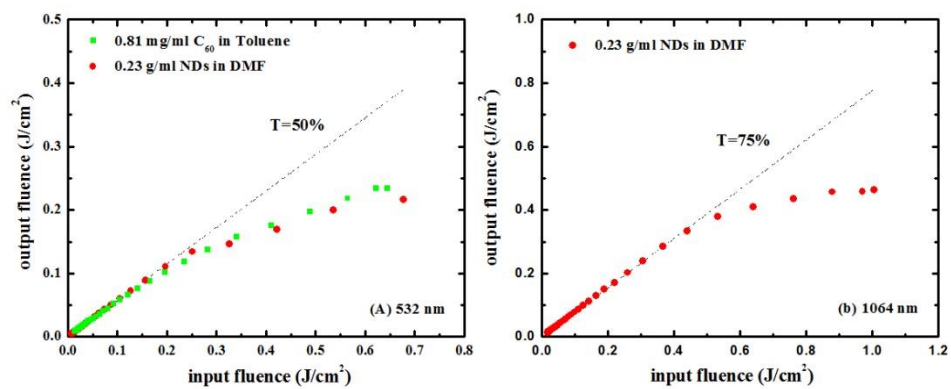


**Fig. 8** Optical limiting of a 0.23 g/ml suspension of NDs in DMF and of a 0.81 mg/ml C<sub>60</sub>-toluene solution under 4 ns, 532 nm (A) and 1064 nm (B) laser excitation.